

Grams: Gradient Descent with Adaptive Momentum Scaling

Yang Cao*

Xiaoyu Li†

Zhao Song‡

Abstract

We introduce **Gradient Descent with Adaptive Momentum Scaling (Grams)**, a novel optimization algorithm that decouples the direction and magnitude of parameter updates in deep learning. Unlike traditional optimizers that directly integrate momentum into updates, Grams separates the update direction, derived from current gradients, from momentum, which is used solely for adaptive magnitude scaling. This approach enables Grams to achieve improved loss descent compared to state-of-the-art cautious and momentum-based optimizers. We establish a global convergence guarantee for Grams and validate its effectiveness through extensive empirical evaluations. The results demonstrate Grams' superior performance, including faster convergence and better generalization, compared to widely-used optimizers such as Adam, Lion, and their cautious variants. Our results highlight Grams' potential as a transformative approach for efficient optimization in large-scale machine learning.

*ycao4@wyomingseminary.org. Wyoming Seminary.

†7.xiaoyu.li@gmail.com. Independent Researcher.

‡magic.linuxkde@gmail.com. Simons Institute for the Theory of Computing, University of California, Berkeley.

Contents

1	Introduction	2
2	Related Work	3
3	Preliminaries	4
3.1	Notations	5
3.2	Backgrounds on Optimization	5
3.3	Useful Facts	5
3.4	Sign Function and its Properties	7
3.5	Adam Optimizer	8
3.6	Lion Optimizer	8
3.7	Cautious Optimizers	9
3.8	Hamiltonian Descent	12
4	Gradient Descent with Adaptive Momentum Scaling	13
4.1	Definitions	13
4.2	Loss Descent	14
4.3	Hamiltonian Dynamics	16
4.4	Global Convergence of Grams	18
4.4.1	Assumptions	18
4.4.2	Convergence	19
5	Empirical Experiments	20
5.1	Pre-Training	20
5.2	Fine-Tuning	22
6	Conclusion and Future Work	22
A	Experiments Details	27
A.1	Pre-Training	27
A.2	Fine-Tuning	27

1 Introduction

Optimization plays a pivotal role in modern machine learning, serving as the cornerstone for training and fine-tuning models across diverse applications. Over the past decade, the introduction of adaptive optimizers like Adam [KB14] and its variant AdamW [LH17] has significantly shaped the landscape of optimization. These algorithms have become the de facto choices for a variety of tasks, ranging from pre-training Large Language Models (LLMs) [TLI⁺23] to fine-tuning models for text-to-image diffusion [RBL⁺22]. Despite the advent of new methods, AdamW has maintained its dominance, particularly in large-scale training regimes, thanks to its robust convergence properties and general applicability.

The era of LLMs has ushered in unprecedented scaling of model sizes, demanding billions or even trillions of parameters [AAA⁺23]. This scaling places an immense burden on computational resources, intensifying the need for efficient optimization strategies. A faster optimizer directly translates to the ability to process more training tokens within a fixed time budget, leading to the development of more capable models [KMH⁺20]. This necessity has rekindled interest in identifying optimizers that can surpass AdamW in terms of speed, memory efficiency, and convergence guarantees.

Recent innovations, such as SHAMPOO [GKS18], Schedule Free [DYM⁺24], Lion [CLH⁺24], SOAP [VMZ⁺24], and ADOPT [THM⁺24], have pushed the boundaries of optimization by introducing novel update rules, momentum mechanisms, and regularization techniques. These methods promise substantial improvements in training efficiency and model performance, particularly in specialized scenarios. The cautious [LCLL24] mechanism addresses optimization challenges by adaptively masking the momentum term u_t to align with the gradient g_t , preventing conflicts that hinder training. This approach extends to Adam and Lion, resulting in variants like Cautious Adam (C-Adam) and Cautious Lion (C-Lion).

In this paper, we propose Gradient Descent with Adaptive Momentum Scaling (Grams), a novel optimization algorithm designed to address the limitations of existing methods. Unlike traditional optimizers that directly couple momentum with gradient updates, Grams decouples the direction and magnitude of parameter updates. This approach allows the update direction to be derived solely from current gradients, while momentum is utilized to scale the update magnitude. Such decoupling enhances stability and robustness, particularly in dynamic optimization landscapes.

Figure 1 illustrates the superior convergence properties of Grams compared to other state-of-the-art optimizers on a simple convex function. In the left graph, the optimization trajectories of Grams exhibit a combination of characteristics observed in Lion and C-Adam. Specifically, Grams follows a shortcut-like path similar to C-Adam while also demonstrating a zigzagging behavior reminiscent of Lion. However, unlike Lion, which deviates significantly from the optimal path due to its pronounced zigzagging updates, Grams maintains a more controlled trajectory, effectively balancing stability and efficiency during optimization. The middle graph illustrates the logarithmic distance of the weights w_1 and w_2 from the optimum. Here, Grams consistently demonstrates a faster descent compared to other optimizers, indicating superior efficiency in reducing the distance to the optimal solution. The right graph displays the convergence of the objective function value over training steps, where Grams achieves a notably faster reduction and lower final objective value than its competitors. These results collectively underscore Grams' ability to navigate the optimization landscape effectively, outperforming traditional and cautious optimizers in terms of speed and precision, even in a simple convex setting.

Our contributions are summarized as follows:

- We introduce the Grams optimizer, which empirically outperforms existing methods such as

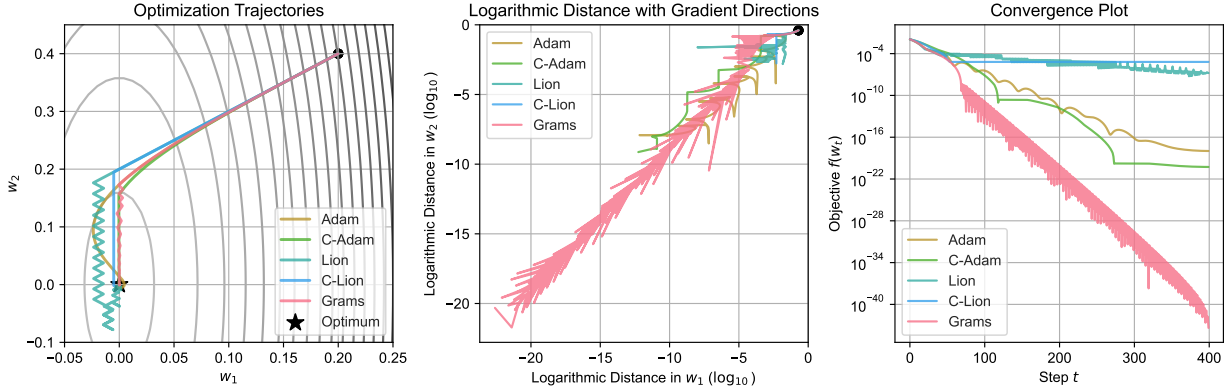


Figure 1: Converging comparison on a simple convex function $f(w) := (0.5w_1)^2 + (0.1w_2)^2$. Learning rate $\eta = 0.01$ for Grams, Adam and C-Adam, and $\eta = 0.001$ for Lion and C-Lion. β_1 and β_2 are default values for all optimizers. The graph in the left is the optimizing trajectories; graph in the middle graph is the distance between current weight and optimum weight; graph in the right is the training objectives.

Adam [LH17], Lion [CLH⁺24] and their Cautious version [LCLL24].

- We establish theoretical guarantees for Grams, including discrete-time descent analysis and Hamiltonian descent analysis.
- We demonstrate the global convergence property of Grams in specific optimization problems under the standard assumptions.

By integrating insights from momentum-based methods, adaptive optimizers, and sign-based updates, Grams bridges the gap between theoretical rigor and practical performance, offering a promising direction for scalable and efficient optimization in modern machine learning.

Roadmap. In Section 2, we review related work and place our approach in the context of existing optimization methods. In Section 3, we introduce our notation system and outline key preliminary concepts necessary for understanding our method. In Section 4, we present our main contribution, Gradient Descent with Adaptive Momentum Scaling (Grams), and provide theoretical guarantees for its performance. In Section 5, we evaluate the effectiveness of Grams through empirical experiments on both pre-training and fine-tuning tasks, comparing its performance to state-of-the-art optimizers. In Section 6, we conclude the paper and discuss future directions to further enhance the capabilities of Grams.

2 Related Work

Adam Variants and Memory-Efficient Optimization Adam and its numerous variants have been pivotal in addressing optimization challenges across diverse applications [KB14, LOG⁺19]. Among these, AdamW [LOG⁺19] introduced a crucial modification by decoupling weight decay from gradient updates, restoring the original intent of weight regularization. NAdam [Doz16] integrated Nesterov momentum, and AdaBelief [ZTD⁺20] refined the second moment estimation for improved generalization. Adan [XZL⁺24] extended these advancements with an additional momentum

term, balancing performance with memory overhead. Schedule-free optimizers [DYM+24] have further simplified the optimization process by dynamically adjusting learning rates without pre-defined schedules, enhancing adaptability across tasks. More recent efforts, such as ADOPT [THM+24], streamlined first-order momentum updates through normalization.

Memory-efficient strategies have addressed the growing resource demands of large-scale models. AdaFactor [SS18] factorize second-order statistics, achieving sublinear memory usage. K-Fac [MG15] approximates the Fisher information matrix using Kronecker-factored representations. Innovations such as fused gradient computation [LYL+23] and GaLore [ZZC+24] leverage low-rank gradient structures to optimize memory efficiency.

Regularization Techniques Regularization plays a critical role in improving generalization and robustness in optimization. Lion [CLH+24] introduced sign-based updates with uniform magnitudes, offering inherent noise regularization [NVL+17, FKMN21, CHG22]. Earlier methods, such as signSGD [BWAA18], explored similar ideas but focused on reducing communication costs in distributed optimization. Despite its efficiency, signSGD often underperformed in deep learning tasks, such as ConvNet training, where Lion demonstrated superior performance through advanced momentum mechanisms.

Building on these ideas, the Cautious mechanism [LCLL24] adaptively masks momentum terms to ensure alignment with gradient directions, mitigating conflicts. This approach has led to new variants, including Cautious Adam (C-Adam) and Cautious Lion (C-Lion), which combine regularization benefits with robust convergence guarantees.

Hamiltonian Dynamics in Optimization Hamiltonian dynamics provides a robust theoretical framework for understanding momentum-based optimization [Nes83, SMDH13, NCLL24, Ano24]. The seminal work of [SMDH13] provided a physical interpretation of momentum methods, linking the oscillatory behavior of algorithms like Nesterov’s and Polyak’s methods [Nes83] to principles of dynamical systems. While traditional gradient descent guarantees a monotonic decrease in objective function values, momentum-based methods exhibit non-monotonic dynamics that require more advanced analytical tools [JNJ18]. This has motivated the development of Lyapunov-based approaches for convergence analysis in convex optimization [KBB15, WRJ16].

Recent studies have further formalized these connections by modeling optimization processes as continuous-time ODEs, uncovering inherent Hamiltonian structures [MPT+18, NCLL24]. These insights have significantly enhanced the theoretical understanding of classical momentum-based algorithms and provided a foundation for exploring new optimization frameworks [Ano24]. Moreover, Hamiltonian principles have been extended to analyze convergence rates for accelerated methods [JNJ18] and have inspired broader applications in optimization. In parallel, Mirror Descent, while distinct from Hamiltonian dynamics, leverages variational principles and maintains efficiency with a mild dependence on the dimensionality of decision variables, making it well-suited for large-scale problems [KBB15, TRRB23].

3 Preliminaries

In this section, we outline foundational concepts and notations that will be referenced throughout the paper. In Section 3.1, we define some useful notations. In Section 3.2 provides essential definitions in optimization, which are critical for understanding the theoretical guarantees of our proposed method. Section 3.3 highlights useful mathematical properties that facilitate the development and analysis of the Grams algorithm. In Section 3.5, 3.6 and 3.7, we review key optimizers,

including Adam [LH17], Lion [CLH+24], and the cautious mechanism [LCLL24]. In Section 3.8, we summarize the Hamiltonian dynamics framework, which provides a theoretical foundation for understanding momentum-based optimization algorithms.

3.1 Notations

For two vectors $u, v \in \mathbb{R}^d$, we use $\langle u, v \rangle$ to denote the standard inner product in the Euclidean space. We use $\|u\|_2$ to denote the ℓ_2 -norm of u and use $\|u\|_\infty$ to denote the ℓ_∞ -norm of u . For a matrix A , we use $\|A\|_F$ to denote the Frobenius norm of A . For a twice differentiable function $f : \mathbb{R}^d \rightarrow \mathbb{R}$, we use $\nabla f(x)$ and $\nabla^2 f(x)$ to denote the gradient and Hessian of f , respectively. Given a vector $x \in \mathbb{R}^d$, we use $\mathbf{1}_{x \geq 0} \in \mathbb{R}^d$ to denote the vector where each entry indicates whether the corresponding entry of x is non-negative, i.e., for each $i \in [d]$, $(\mathbf{1}_{x \geq 0})_i = 1$ if $x_i \geq 0$, and $(\mathbf{1}_{x \geq 0})_i = 0$ otherwise.

3.2 Backgrounds on Optimization

We define the L -smoothness of functions as below.

Definition 3.1 (L -smooth). *We say that a function $f : \mathbb{R}^d \rightarrow \mathbb{R}$ is L -smooth if $\|\nabla f(x_1) - \nabla f(x_2)\|_2 \leq L\|x_1 - x_2\|_2$ for all $x_1, x_2 \in \mathbb{R}^d$.*

We state a common fact of L -smooth functions as follow.

Fact 3.2. *If a function $f : \mathbb{R}^d \rightarrow \mathbb{R}$ is L -smooth, then we have*

$$\begin{aligned} f(x_2) &\leq f(x_1) + \langle \nabla f(x_1), x_2 - x_1 \rangle + \frac{L}{2} \|x_2 - x_1\|_2^2, \\ f(x_2) &\geq f(x_1) + \langle \nabla f(x_1), x_2 - x_1 \rangle - \frac{L}{2} \|x_2 - x_1\|_2^2. \end{aligned}$$

We also define PL-condition as below.

Definition 3.3 (PL-condition). *A function $f : \mathbb{R}^d \rightarrow \mathbb{R}$ satisfies the μ -Polyak-Lojasiewicz (PL) condition with constant $\mu > 0$ if the following inequality holds for all $x \in \mathbb{R}^d$:*

$$\|\nabla f(x)\|^2 \geq 2\mu(f(x) - f^*),$$

where f^* is the minimum value of the function f , i.e., $f^* = \inf_{x \in \mathbb{R}^d} f(x)$.

3.3 Useful Facts

We introduce some useful facts, which plays crucial roles in the later proofs.

Fact 3.4. *Given vectors $a, b, c \in \mathbb{R}^d$, we have*

$$\langle a, b \circ c \rangle = \langle a \circ b, c \rangle.$$

Fact 3.5. *Let two vectors $a, b \in \mathbb{R}^n$, then:*

$$\langle a, -\text{sign}(a) \circ |b| \rangle = \langle |a|, |b| \rangle$$

Proof. For the left side of the equation:

$$\begin{aligned}\langle a, -\text{sign}(a) \circ |b| \rangle &= \sum_{i=1}^n -a_i \text{sign}(a_i) |b|_i \\ &= - \sum_{i=1}^n |a_i| |b|_i \\ &= - \langle |a|, |b| \rangle\end{aligned}$$

where the first step comes from the definition of inner product, the second step uses Fact 3.9, and the final step uses the definition of inner product again. \square

Fact 3.6. Let two vectors $a, b \in \mathbb{R}^n$, then:

$$\langle a, b \rangle - \langle |a|, |b| \rangle \leq 0.$$

Proof.

$$\begin{aligned}\langle a, b \rangle - \langle |a|, |b| \rangle &= \sum_{i=1}^n a_i b_i - |a_i| |b|_i \\ &= \sum_{i=1}^n \begin{cases} 0 & \text{if } a_i \text{ and } b_i \text{ have the same sign} \\ -2|a_i| |b|_i & \text{if } a_i \text{ and } b_i \text{ have opposite signs} \end{cases} \\ &\leq 0,\end{aligned}$$

where the first step uses the definition of inner product, the second step discusses the only two cases we have for signs, and the final inequality comes from basic algebra. \square

Fact 3.7. Let $x = a \circ b$ be an element-wise product of two vectors $a, b \in \mathbb{R}^n$, then:

$$\langle a, b \rangle - \langle |a|, |b| \rangle - \langle a \circ b, \mathbf{1} - \mathbf{1}_{a \circ b > 0} \rangle \leq 0$$

Proof.

$$\begin{aligned}\langle a, b \rangle - \langle |a|, |b| \rangle - \langle a \circ b, \mathbf{1} - \mathbf{1}_{a \circ b > 0} \rangle &= \sum_{i=1}^n a_i b_i - \sum_{i=1}^n |a_i| |b|_i - \left(\sum_{i=1}^n a_i b_i - \sum_{i: a_i b_i > 0} a_i b_i \right) \\ &= \sum_{i: a_i b_i > 0} a_i b_i - \sum_{i=1}^n |a_i| |b|_i,\end{aligned}$$

where the first step expands the terms, and the second step simplifies by splitting the sum based on the sign of $a_i b_i$.

If all $a_i b_i \geq 0$, then $\sum_{i: a_i b_i > 0} a_i b_i = \sum_{i=1}^n |a_i| |b|_i$, so the expression is 0. Otherwise, $\sum_{i=1}^n |a_i| |b|_i > \sum_{i: a_i b_i > 0} a_i b_i$, so the expression is negative.

Thus,

$$\langle a, b \rangle - \langle |a|, |b| \rangle - \langle a \circ b, \mathbf{1}_d - \mathbf{1}_{a \circ b > 0} \rangle = \sum_{i: a_i b_i > 0} a_i b_i - \sum_{i=1}^n |a_i| |b|_i \leq 0.$$

The proof is complete. \square

3.4 Sign Function and its Properties

We formally define the sign function, which will be used later in our optimizer Grams.

Definition 3.8 (Sign function). *Given a vector $a = (a_1, a_2, \dots, a_n) \in \mathbb{R}^n$, the sign function of a , denoted as $\text{sign}(a)$, is defined component-wise as:*

$$\text{sign}(a) = (\text{sign}(a_1), \text{sign}(a_2), \dots, \text{sign}(a_n)),$$

where the scalar sign function $\text{sign}(a_i)$ is given by:

$$\text{sign}(a_i) = \begin{cases} 1, & \text{if } a_i > 0, \\ 0, & \text{if } a_i = 0, \\ -1, & \text{if } a_i < 0. \end{cases}$$

We list some property of sign function below, which will be used in later proofs.

Fact 3.9. *Given a scalar $a \in \mathbb{R}$, we have:*

$$a \cdot \text{sign}(a) = |a|.$$

Proof. Let $a \in \mathbb{R}$. By Definition 3.8:

$$\text{sign}(a) = \begin{cases} 1, & \text{if } a > 0, \\ 0, & \text{if } a = 0, \\ -1, & \text{if } a < 0. \end{cases}$$

Consider the following cases:

- If $a > 0$, then $\text{sign}(a) = 1$, so:

$$a \cdot \text{sign}(a) = a \cdot 1 = a = |a|.$$

- If $a = 0$, then $\text{sign}(a) = 0$, so:

$$a \cdot \text{sign}(a) = 0 \cdot 0 = 0 = |a|.$$

- If $a < 0$, then $\text{sign}(a) = -1$, so:

$$a \cdot \text{sign}(a) = a \cdot (-1) = -a = |a|.$$

Thus, in all cases, $a \cdot \text{sign}(a) = |a|$. □

Fact 3.10. *Given a vector $a = (a_1, a_2, \dots, a_n) \in \mathbb{R}^n$, we have:*

$$a \circ \text{sign}(a) = |a|,$$

where the operations are applied component-wise.

Proof. Let $a = (a_1, a_2, \dots, a_n) \in \mathbb{R}^n$. By Definition 3.8, the sign function is applied component-wise:

$$\text{sign}(a) = (\text{sign}(a_1), \text{sign}(a_2), \dots, \text{sign}(a_n)).$$

Expanding the Hadamard product $a \circ \text{sign}(a)$ component-wise:

$$a \circ \text{sign}(a) = (a_1 \cdot \text{sign}(a_1), a_2 \cdot \text{sign}(a_2), \dots, a_n \cdot \text{sign}(a_n)).$$

By Fact 3.9 (the scalar version), for each i :

$$a_i \cdot \text{sign}(a_i) = |a_i|.$$

Thus:

$$a \circ \text{sign}(a) = (|a_1|, |a_2|, \dots, |a_n|) = |a|,$$

where the absolute value $|a|$ is applied component-wise. □

3.5 Adam Optimizer

Adam (Adaptive Moment Estimation) [KB14] is a widely-used optimizer that combines the benefits of RMSprop [HSS12] and momentum by maintaining both first and second moment estimates of the gradients. The algorithm adapts the learning rates for each parameter using these estimates.

Definition 3.11 (Adam). *The parameter update rule for Adam is given by:*

$$\begin{aligned} m_t &:= \beta_1 m_{t-1} + (1 - \beta_1) g_t \\ v_t &:= \beta_2 v_{t-1} + (1 - \beta_2) g_t^2 \\ \widehat{m}_t &:= \frac{m_t}{1 - \beta_1^t} \\ \widehat{v}_t &:= \frac{v_t}{1 - \beta_2^t} \\ u_t &:= \frac{\widehat{m}_t}{\sqrt{\widehat{v}_t} + \epsilon} \\ w_{t+1} &:= w_t - \eta_t u_t, \end{aligned}$$

where w_t is the weight at time step t , m_t and v_t are the first and second moment estimates respectively, $g_t = \nabla_w \mathcal{L}_t(w_{t-1})$ is the current gradient, β_1 and β_2 are decay rates for the moment estimates, ϵ is a small constant for numerical stability, and η_t is the learning rate at step t .

3.6 Lion Optimizer

Evolved Sign Momentum (Lion) [CLH⁺24] is an efficient optimizer that leverages momentum and sign-based updates. Lion's key innovation lies in its update rule, which combines both current and momentum gradients through sign operations.

Definition 3.12 (Lion Parameter Update). *The parameter update rule for Lion is given by:*

$$u_t := \text{sign}(\beta_1 m_{t-1} + (1 - \beta_1) g_t)$$

Algorithm 1 Adam [KB14]

Require: parameter w , step sizes $\{\eta_t\}$, dampening factors $\beta_1, \beta_2 \in [0, 1)$, $\epsilon > 0$, weight decay $\gamma \geq 0$

- 1: Initialize $t = 0$, $m_0 = v_0 = \mathbf{0}$
 - 2: **while** w_t not converged **do**
 - 3: $t \leftarrow t + 1$
 - 4: $g_t \leftarrow \nabla_w \mathcal{L}_t(w_{t-1})$
 - 5: $m_t \leftarrow \beta_1 m_{t-1} + (1 - \beta_1) g_t$
 - 6: $v_t \leftarrow \beta_2 v_{t-1} + (1 - \beta_2) g_t^2$
 - 7: $\widehat{m}_t \leftarrow m_t / (1 - \beta_1^t)$
 - 8: $\widehat{v}_t \leftarrow v_t / (1 - \beta_2^t)$
 - 9: $u_t \leftarrow \widehat{m}_t / (\sqrt{\widehat{v}_t} + \epsilon)$
 - 10: $w_t \leftarrow w_{t-1} - \epsilon_t u_t$
 - 11: $w_t \leftarrow w_t - \epsilon_t \gamma w_t$ ▷ Add weight decay [LH17]
 - 12: **end while**
-

$$\begin{aligned} w_t &:= w_{t-1} - \eta_t \cdot u_t \\ m_t &:= \beta_2 m_{t-1} + (1 - \beta_2) g_t, \end{aligned}$$

where w_t is the weight at time step t , m_{t-1} is the momentum term, $g_t = \nabla_w \mathcal{L}_t(w_{t-1})$ is the current gradient, β_1 and β_2 are the momentum coefficients, η_t is the learning rate at step t , and sign is defined in Definition 3.8,

Lion’s efficiency stems from its memory-efficient design - it only needs to maintain a single momentum term and operates primarily through sign operations. This makes it particularly suitable for large-scale training where memory constraints are significant. The optimizer has demonstrated strong performance in training large language models and vision transformers, often achieving comparable or better results than Adam while using less memory.

3.7 Cautious Optimizers

Cautious mechanism [LCLL24] addresses a key challenge in optimization dynamics: when the momentum term u_t moves in a different direction from the current gradient g_t , it can potentially impede training progress. To mitigate this issue, Cautious mechanism introduces an adaptive masking mechanism that modifies the momentum term based on its alignment with the gradient direction. Cautious mechanism could apply to Adam and Lion, which form Cautious Adam (C-Adam) and Cautious Lion (C-Lion).

Definition 3.13 (Cautious Mechanism Parameter Update). *The general parameter update rule for Cautious mechanism is given by:*

$$\begin{aligned} \widehat{u}_t &:= u_t \circ \mathbf{1}_{u_t \circ g_t \geq 0} \\ w_t &:= w_{t-1} - \eta_t \widehat{u}_t, \end{aligned} \tag{1}$$

where w_t is the weight at time step t , \circ denotes Hadamard product. For C-Adam, u_t is from Definition 3.11; For C-Lion, u_t is from Definition 3.12. g_t is the current gradient.

The cautious mechanism in Definition 3.13 modifies the parameter updates to ensure they align with the gradient direction, thereby reducing the risk of adverse updates that could impede convergence. To analyze the impact of this mechanism, we introduce Definition 3.14, which quantifies the change in the loss function after an update.

Definition 3.14. For any loss function $\mathcal{L} : \mathbb{R}^d \rightarrow \mathbb{R}$, we define

$$\Delta\mathcal{L}_{w_{t+1}, w_t} := \mathcal{L}(w_{t+1}) - \mathcal{L}(w_t)$$

where w_{t+1} is updated from any update rule.

Algorithm 2 Cautious Adam (C-Adam) [LCLL24]

Require: parameter w , step sizes $\{\eta_t\}$, dampening factors $\beta_1, \beta_2 \in [0, 1)$, $\epsilon > 0$, weight decay $\gamma \geq 0$

- 1: Initialize $t = 0$, $m_0 = v_0 = \mathbf{0}$
 - 2: **while** w_t not converged **do**
 - 3: $t \leftarrow t + 1$
 - 4: $g_t \leftarrow \nabla_w \mathcal{L}_t(w_{t-1})$
 - 5: $m_t \leftarrow \beta_1 m_{t-1} + (1 - \beta_1) g_t$
 - 6: $v_t \leftarrow \beta_2 v_{t-1} + (1 - \beta_2) g_t^2$
 - 7: $\hat{m}_t \leftarrow m_t / (1 - \beta_1^t)$
 - 8: $\hat{v}_t \leftarrow v_t / (1 - \beta_2^t)$
 - 9: $u_t \leftarrow \hat{m}_t / (\sqrt{\hat{v}_t} + \epsilon)$
 - 10: $\phi_t \leftarrow \mathbf{1}_{u_t \circ g_t \geq 0}$ ▷ Compute alignment mask
 - 11: $\bar{\eta}_t = \eta_t \frac{d}{\|\phi_t\|_0 + 1}$ ▷ Scale lr, d is dimension of ϕ_t
 - 12: $w_t \leftarrow w_{t-1} - \bar{\eta}_t \phi_t \circ u_t$
 - 13: $w_t \leftarrow w_t - \bar{\eta}_t \gamma w_t$ ▷ Add weight decay [LH17]
 - 14: **end while**
-

As shown in [LCLL24], the cautious mechanism ensures that the updated parameters result in a non-negative inner product with the gradient, leading to a monotonic decrease in the loss function when the step size is sufficiently small. Specifically, using a Taylor approximation, it can be expressed as:

$$\Delta\mathcal{L}_{w_{t+1}, w_t} \approx -\eta_t (u_t \circ g_t)^\top \phi(u_t \circ g_t) \leq 0,$$

where $\phi(\cdot)$ represents the alignment mask introduced by the cautious mechanism. This guarantees that $\mathcal{L}(w_{t+1}) \leq \mathcal{L}(w_t)$, ensuring a decrease in loss.

We formalize that the expected decrease in loss when updating the parameter w from optimization step t to step $t + 1$ can be approximated using a first-order Taylor expansion, which indicates the loss function will decrease monotonically when the step size is sufficiently small.

Lemma 3.15. Suppose that $\mathcal{L} : \mathbb{R}^d \rightarrow \mathbb{R}$ is L -smooth. Let $\Delta\mathcal{L}_{w_{t+1}, w_t}^C$ be defined in Definition 3.14, w_{t+1}^C is updated from w_t using Definition 3.13. Then we have the followings:

- Part 1. It holds that

$$\Delta\mathcal{L}_{w_{t+1}, w_t}^C \leq -\eta_t \langle u_t \circ g_t, \mathbf{1}_{u_t \circ g_t \geq 0} \rangle + \frac{L\eta_t^2}{2} \|u_t\|_2^2, \quad (2)$$

- Part 2. It holds that

$$\Delta\mathcal{L}_{w_{t+1}, w_t}^C \geq -\eta_t \langle u_t \circ g_t, \mathbf{1}_{u_t \circ g_t \geq 0} \rangle.$$

- Part 3. If $\eta_t \leq \frac{2}{L\|u_t\|_2^2} \langle u_t \circ g_t, \mathbf{1}_{u_t \circ g_t \geq 0} \rangle$, then $\Delta\mathcal{L}_{w_{t+1}, w_t}^C \leq 0$.

Proof. Proof of Part 1. We can show that

$$\begin{aligned}
\Delta \mathcal{L}_{w_{t+1}, w_t}^C &= \mathcal{L}(w_{t+1}) - \mathcal{L}(w_t) \\
&\leq \mathcal{L}(w_t) + \langle g_t, w_{t+1} - w_t \rangle + \frac{L}{2} \|w_{t+1} - w_t\|_2^2 - \mathcal{L}(w_t) \\
&= \langle g_t, w_{t+1} - w_t \rangle + \frac{L}{2} \|w_{t+1} - w_t\|_2^2 \\
&= \langle g_t, -\eta_t u_t \circ \mathbf{1}_{u_t \circ g_t \geq 0} \rangle + \frac{L}{2} \|\eta_t u_t \circ \mathbf{1}_{u_t \circ g_t \geq 0}\|_2^2 \\
&= -\eta_t \langle u_t \circ g_t, \mathbf{1}_{u_t \circ g_t \geq 0} \rangle + \frac{L}{2} \|\eta_t u_t \circ \mathbf{1}_{u_t \circ g_t \geq 0}\|_2^2 \\
&\leq -\eta_t \langle u_t \circ g_t, \mathbf{1}_{u_t \circ g_t \geq 0} \rangle + \frac{L\eta_t^2}{2} \|u_t\|_2^2
\end{aligned} \tag{3}$$

where the first step follows from Definition 3.14, the second step follows from that \mathcal{L} is L -smooth and Fact 3.2, the third step follows from basic algebra, the fourth step follows from Definition 3.13, the fifth step follows from Fact 3.4, and the last step follows from basic algebra.

Proof of Part 2. Next, we can show that

$$\begin{aligned}
\Delta \mathcal{L}_{w_{t+1}, w_t}^C &= \mathcal{L}(w_{t+1}) - \mathcal{L}(w_t) \\
&\geq \mathcal{L}(w_t) + \langle g_t, w_{t+1} + w_t \rangle - \frac{L}{2} \|w_{t+1} - w_t\|_2^2 - \mathcal{L}(w_t) \\
&\geq \langle g_t, w_{t+1} - w_t \rangle \\
&= \langle g_t, -\eta_t u_t \circ \mathbf{1}_{u_t \circ g_t \geq 0} \rangle \\
&= -\eta_t \langle u_t \circ g_t, \mathbf{1}_{u_t \circ g_t \geq 0} \rangle
\end{aligned} \tag{4}$$

where the first step follows from Definition 3.14, the second step follows from that \mathcal{L} is L -smooth and Fact 3.2, the third step follows from basic algebra, the fourth step follows from Definition 3.13, the last step follows from Fact 3.4.

Proof of Part 3. By rearranging the Eq. (3), it is clear that if $\eta_t \leq \frac{2}{L\|u_t\|_2^2} \langle u_t \circ g_t, \mathbf{1}_{u_t \circ g_t \geq 0} \rangle$, then we have $\Delta \mathcal{L}_{w_{t+1}, w_t}^C \leq 0$. \square

Building on these findings, Theorem 3.16 delves into the Hamiltonian properties of the cautious mechanism, providing deeper insights into its theoretical guarantees within continuous optimization dynamics.

Theorem 3.16 (Theorem 2.3 in [LCLL24]). *For Hamiltonian dynamics of Cautious optimizer (in Definition 3.13), we have:*

$$\begin{aligned}
\Delta_H^C(w_t, s_t) &:= \frac{d}{dt} H(w_t, s_t) = \langle x_t, \mathbf{1} - \mathbf{1}_{x_t > 0} \rangle - \Delta_H(w_t, s_t). \\
\Delta_{\mathcal{L}}^C(w_t, s_t) &:= \frac{d}{dt} \mathcal{L}(w_t) = -\langle x_t, \mathbf{1}_{x_t > 0} \rangle - \langle \nabla \mathcal{L}(w_t), \Phi_t(\nabla \mathcal{L}(w_t)) \rangle \\
&= \langle x_t, \mathbf{1} - \mathbf{1}_{x_t > 0} \rangle - \Delta_{\mathcal{L}}(w_t, s_t).
\end{aligned}$$

where $\Delta_{H_t}(w_t, s_t)$ and $\Delta_{\mathcal{L}_t}(w_t, s_t)$ represent the decreasing rates of H and \mathcal{L} in accordance with the system in Definition 3.17.

Hence:

- If $\langle x_t, (\mathbf{1}_d - \text{sign}(x_t)) \rangle \leq 0$ for any $x \in \mathbb{R}^d$, then both H and \mathcal{L} decrease faster than the original system:

$$\begin{aligned}\Delta_H^C(w_t, s_t) &\leq -\Delta_{H_t}(w_t, s_t) \leq 0, \\ \Delta_{\mathcal{L}}^C(w_t, s_t) &\leq -\Delta_{\mathcal{L}_t}(w_t, s_t).\end{aligned}$$

- If $\langle x_t, \text{sign}(\nabla \mathcal{L}(w_t)) \rangle \geq 0$ for any $x \in \mathbb{R}^d$, then \mathcal{L} decreases monotonically:

$$\Delta_{\mathcal{L}}^C(w_t, s_t) \leq 0.$$

3.8 Hamiltonian Descent

Hamiltonian descent provides a theoretical framework for analyzing momentum-based optimization algorithms by introducing an augmented objective function, the Hamiltonian. This framework allows us to study optimization dynamics through the lens of continuous-time differential equations, linking the monotonic descent of the Hamiltonian function to the stability and convergence of the optimization process. Below, we formalize this concept based on the formulation presented in Section 2.1 of [LCLL24].

Definition 3.17 (Section 2.1 from [LCLL24]). *Momentum-based algorithms can be typically viewed as monotonic descending algorithms on an augmented loss $H(W, S)$, which satisfies $\min_S H(W, S) = \mathcal{L}(W)$, so that minimizing $\mathcal{L}(W)$ is equivalent to minimizing $H(W, S)$. A typical choice is*

$$H(w, s) = \mathcal{L}(w) + \mathcal{K}(s),$$

where $\mathcal{K}(\cdot)$ is any lower bounded function. The continuous-time form of most momentum-based algorithms can be written into a Hamiltonian descent form:

$$\begin{aligned}\frac{d}{dt}w_t &= -\nabla \mathcal{K}(s_t) - \Phi_t(\nabla \mathcal{L}(w_t)) \\ \frac{d}{dt}s_t &= \nabla \mathcal{L}(w_t) - \Psi_t(\nabla \mathcal{K}(s_t))\end{aligned}\tag{5}$$

where $H(W, S)$ is a Hamiltonian (or Lyapunov) function that satisfies

$$\min_S H(W, S) = \mathcal{L}(W), \quad \forall W,$$

so that minimizing $\mathcal{L}(W)$ reduces to minimizing $H(W, S)$; and $\Phi(\cdot), \Psi(\cdot)$ are two monotonic mappings satisfying

$$\langle x, \Phi(x) \rangle \geq 0, \quad \langle x, \Psi(x) \rangle \geq 0, \quad \forall x \in X.$$

With $\Phi(X) = \Psi(X) = 0$, the system in (5) reduces to the standard Hamiltonian system that keeps $H(W_t, S_t) = \text{const}$ along the trajectory. When adding the descending components with Φ and Ψ , the system then keeps $H(W, S)$ monotonically decreasing:

$$\frac{d}{dt}H(w_t, s_t) = \Delta_H(w_t, s_t) \leq 0,$$

where

$$\Delta_H(w_t, s_t) := -\langle x, \Phi(x) \rangle - \langle x, \Psi(x) \rangle.\tag{6}$$

On the other hand, $\mathcal{L}(w)$, which is the true objective, is not necessarily decreasing monotonically.

$$\frac{d}{dt}\mathcal{L}(w_t) = -\Delta_{\mathcal{L}}(w_t, s_t),$$

where

$$\Delta_{\mathcal{L}}(w_t, s_t) := \langle \nabla \mathcal{L}(w_t), \nabla \mathcal{K}(s_t) \rangle + \langle \nabla \mathcal{L}(w_t), \Phi_t(\nabla \mathcal{L}(w_t)) \rangle.\tag{7}$$

4 Gradient Descent with Adaptive Momentum Scaling

We propose *Gradient Descent with Adaptive Momentum Scaling* (**Grams**). Grams decouples the direction and magnitude of the update by using the direction from gradients while scaling it with the norm of momentum. This section formalizes the Grams update rule, introduces its key components, and provides theoretical guarantees in both loss descent and Hamiltonian dynamics for its performance.

4.1 Definitions

We define the parameter updating rule of Grams formally as below.

Definition 4.1 (Grams Parameter Update). *The parameter update rule for Grams is:*

$$\begin{aligned}
 m_t &:= \beta_1 m_{t-1} + (1 - \beta_1) g_t \\
 v_t &:= \beta_2 v_{t-1} + (1 - \beta_2) g_t^2 \\
 \hat{m}_t &:= \frac{m_t}{1 - \beta_1^t} \\
 \hat{v}_t &:= \frac{v_t}{1 - \beta_2^t} \\
 u_t &:= \frac{\hat{m}_t}{\sqrt{\hat{v}_t} + \epsilon} \\
 \hat{u}_t &:= \text{sign}(g_t) \circ |u_t| \\
 w_t &:= w_{t-1} - \eta_t \hat{u}_t,
 \end{aligned} \tag{8}$$

where w_t is the weight at time step t , $g_t = \nabla_w \mathcal{L}_t(w_{t-1})$ is the current gradient, $|\cdot|$ is element-wise absolute value, \circ denotes Hadamard product, and $\text{sign}(\cdot)$ is defined in Definition 3.8.

Algorithm 3 Gradient Descent with Adaptive Momentum Scaling (Grams)

Require: parameter w , step sizes $\{\eta_t\}$, dampening factors $\beta_1, \beta_2 \in [0, 1)$, $\epsilon > 0$, weight decay

- $\gamma \geq 0$
- 1: Initialize $t = 0$, $m_0 = v_0 = \mathbf{0}$
 - 2: **while** w_t not converged **do**
 - 3: $t \leftarrow t + 1$
 - 4: $g_t \leftarrow \nabla_w \mathcal{L}_t(w_{t-1})$
 - 5: $m_t \leftarrow \beta_1 m_{t-1} + (1 - \beta_1) g_t$
 - 6: $v_t \leftarrow \beta_2 v_{t-1} + (1 - \beta_2) g_t^2$
 - 7: $\hat{m}_t \leftarrow m_t / (1 - \beta_1^t)$
 - 8: $\hat{v}_t \leftarrow v_t / (1 - \beta_2^t)$
 - 9: $u_t \leftarrow \hat{m}_t / (\sqrt{\hat{v}_t} + \epsilon)$
 - 10: $\hat{u}_t \leftarrow \text{sign}(g_t) \circ |u_t|$
 - 11: $w_t \leftarrow w_{t-1} - \eta_t \hat{u}_t$
 - 12: $w_t \leftarrow w_t - \eta_t \gamma w_t$ ▷ Add weight decay [LH17]
 - 13: **end while**
-

4.2 Loss Descent

In this subsection, we analyze the loss descent properties of the Grams algorithm. Understanding how the loss function decreases over optimization steps provides insights into the efficiency and stability of the method. Below, we formalize the relationship between the step size, gradients, and the resulting decrease in the loss value, leveraging the L -smoothness property of the objective function.

Lemma 4.2. *Suppose that $\mathcal{L} : \mathbb{R}^d \rightarrow \mathbb{R}$ is L -smooth. Let $\Delta\mathcal{L}_{w_{t+1}^{\text{Grams}}, w_t}$ be defined in Definition 3.14, w_{t+1}^{Grams} is updated from w_t using Eq. (8). Then we have the following:*

- Part 1. It holds that

$$\Delta\mathcal{L}_{w_{t+1}^{\text{Grams}}, w_t} \leq -\eta_t \langle |g_t|, |u_t| \rangle + \frac{L\eta_t^2}{2} \|u_t\|_2^2. \quad (9)$$

- Part 2. It holds that

$$\Delta\mathcal{L}_{w_{t+1}^{\text{Grams}}, w_t} \geq -\eta_t \langle |g_t|, |u_t| \rangle.$$

- Part 3. If $\eta_t \leq \frac{2}{L\|u_t\|^2} \langle |g_t|, |u_t| \rangle$, then we have $\Delta\mathcal{L}_{w_{t+1}^{\text{Grams}}, w_t} \leq 0$.

Proof. **Proof of Part 1.** We can show that

$$\begin{aligned} \Delta\mathcal{L}_{w_{t+1}^{\text{Grams}}, w_t} &= \mathcal{L}(w_{t+1}) - \mathcal{L}(w_t) \\ &\leq \mathcal{L}(w_t) + \langle g_t, w_{t+1} - w_t \rangle + \frac{L}{2} \|w_{t+1} - w_t\|_2^2 - \mathcal{L}(w_t) \\ &= \langle g_t, w_{t+1} - w_t \rangle + \frac{L}{2} \|w_{t+1} - w_t\|_2^2 \\ &= \langle g_t, -\eta_t \cdot \text{sign}(g_t) \circ |u_t| \rangle + \frac{L}{2} \|\eta_t \cdot \text{sign}(g_t) \circ |u_t|\|_2^2 \\ &= -\eta_t \langle g_t \circ \text{sign}(g_t), |u_t| \rangle + \frac{L}{2} \|\eta_t u_t\|_2^2 \\ &\leq -\eta_t \langle |g_t|, |u_t| \rangle + \frac{L\eta_t^2}{2} \|u_t\|_2^2 \end{aligned} \quad (10)$$

where the first step follows from Definition 3.14, the second step follows from that \mathcal{L} is L -smooth and Fact 3.2, the third step follows from basic algebra, the fourth step follows from Definition 4.1, the fifth step follows from the Fact 3.4, and the last step follows from $g_t \circ \text{sign}(g_t) = |g_t|$.

Proof of Part 2. Next, we can show that

$$\begin{aligned} \Delta\mathcal{L}_{w_{t+1}^{\text{Grams}}, w_t} &= \mathcal{L}(w_{t+1}) - \mathcal{L}(w_t) \\ &\geq \mathcal{L}(w_t) + \langle g_t, w_{t+1} - w_t \rangle - \frac{L}{2} \|w_{t+1} - w_t\|_2^2 - \mathcal{L}(w_t) \\ &\geq \langle g_t, w_{t+1} - w_t \rangle \\ &= \langle g_t, -\eta_t \cdot \text{sign}(g_t) \circ |u_t| \rangle \\ &= -\eta_t \langle |g_t|, |u_t| \rangle \end{aligned} \quad (11)$$

where the first step follows from Definition 3.14, the second step follows from that \mathcal{L} is L -smooth and Fact 3.2, the third step follows from basic algebra, the fourth step follows from Definition 4.1, the last step follows from the Fact 3.4 and Fact 3.10.

Proof of Part 3. By rearranging the Eq. (10), it is clear that if $\eta_t \leq \frac{2}{L\|u_t\|^2} \langle |g_t|, |u_t| \rangle$, then we have $\Delta\mathcal{L}_{w_{t+1}^{\text{Grams}}, w_t} \leq 0$. \square

Then, we compare the loss descent between Grams and C-Adam.

Theorem 4.3 (Loss Descent Comparison). *Suppose that $\mathcal{L} : \mathbb{R}^d \rightarrow \mathbb{R}$ is L -smooth. For any parameter vector w at optimization step t , let w_t^{Grams} and w_t^{C} be the update of Grams in Definition 4.1 and Cautious optimizers in Definition 3.13, respectively. If the stepsize η_t satisfies*

$$\eta_t \leq \frac{2}{L\|u_t\|^2} \cdot \min\{\langle u_t \circ g_t, \mathbf{1}_{u_t \circ g_t \geq 0} \rangle, \langle u_t \circ g_t, \mathbf{1}_{u_t \circ g_t < 0} \rangle\},$$

then we have

$$\Delta \mathcal{L}_{w_{t+1}^{\text{Grams}}, w_t} \leq \Delta \mathcal{L}_{w_{t+1}^{\text{C}}, w_t} \leq 0.$$

Proof. We define the index sets:

$$\begin{aligned} I^+ &= \{i \in [d] : u_{t,i}, g_{t,i} \geq 0\}; \\ I^- &= \{i \in [d] : u_{t,i}, g_{t,i} < 0\}. \end{aligned}$$

By Part 1. of Lemma 4.2, we have

$$\Delta \mathcal{L}_{w_{t+1}^{\text{Grams}}, w_t} \leq -\eta_t \langle |g_t|, |u_t| \rangle + \frac{L\eta_t^2}{2} \|u_t\|_2^2. \quad (12)$$

By Part 2. of Lemma 3.15, we have

$$\Delta \mathcal{L}_{w_{t+1}^{\text{C}}, w_t} \geq -\eta_t \langle u_t \circ g_t, \mathbf{1}_{u_t \circ g_t \geq 0} \rangle. \quad (13)$$

Then we can show that

$$\begin{aligned} \Delta \mathcal{L}_{w_{t+1}^{\text{Grams}}, w_t} - \Delta \mathcal{L}_{w_{t+1}^{\text{C}}, w_t} &\leq -\eta_t \langle |g_t|, |u_t| \rangle + \eta_t \langle u_t \circ g_t, \mathbf{1}_{u_t \circ g_t \geq 0} \rangle + \frac{L\eta_t^2}{2} \|u_t\|_2^2 \\ &= -\eta_t \sum_{i=1}^d |u_{t,i}| |g_{t,i}| + \eta_t \sum_{i \in I^+} u_{t,i} g_{t,i} + \frac{L\eta_t^2}{2} \|u_t\|_2^2 \\ &= -\eta_t \sum_{i \in I^+} |u_{t,i}| |g_{t,i}| - \eta_t \sum_{i \in I^-} |u_{t,i}| |g_{t,i}| + \eta_t \sum_{i \in I^+} u_{t,i} g_{t,i} + \frac{L\eta_t^2}{2} \|u_t\|_2^2 \\ &= -\eta_t \sum_{i \in I^+} u_{t,i} g_{t,i} - \eta_t \sum_{i \in I^-} |u_{t,i}| |g_{t,i}| + \eta_t \sum_{i \in I^+} u_{t,i} g_{t,i} + \frac{L\eta_t^2}{2} \|u_t\|_2^2 \\ &= -\eta_t \sum_{i \in I^-} |u_{t,i}| |g_{t,i}| + \frac{L\eta_t^2}{2} \|u_t\|_2^2 \end{aligned}$$

where the first step follows from Eq. (13) and Eq. (12), the second step expands vectors element-wise, the third step follows from that $[d]$ is the disjoint union of I^+ and I^- , the fourth step follows from that $|u_{t,i}| |g_{t,i}| = u_{t,i} g_{t,i}$ for $i \in I^+$, and the last step follows from basic algebra.

To ensure $\Delta \mathcal{L}_{w_{t+1}^{\text{Grams}}, w_t} - \Delta \mathcal{L}_{w_{t+1}^{\text{C}}, w_t} \leq 0$, it suffices to have

$$-\eta_t \sum_{i \in I^-} |u_{t,i}| |g_{t,i}| + \frac{L\eta_t^2}{2} \|u_t\|_2^2 \leq 0.$$

Rearranging the above inequality gives

$$\begin{aligned}\eta_t &\leq \frac{2}{L\|u_t\|_2^2} \sum_{i \in I^-} |u_{t,i}| |g_{t,i}| \\ &= \frac{2}{L\|u_t\|_2^2} \langle g_t \circ u_t, \mathbf{1}_{u_t \circ g_t < 0} \rangle,\end{aligned}$$

where the last step follows from the definition of I^- and basic algebra.

Note that by Part 3 of Lemma 3.15, if $\eta_t \leq \frac{2}{L\|u_t\|_2^2} \langle g_t \circ u_t, \mathbf{1}_{g_t \circ u_t \geq 0} \rangle$, we have $\mathcal{L}_{w_{t+1}, w_t}^c \leq 0$. \square

Remark 4.4. *Theorem 4.3 shows that Grams achieves strictly better descent in the loss landscape in the discrete analysis compared to Cautious optimizers. This theoretical guarantee suggests that Grams may converge faster and achieve better minima in practice.*

4.3 Hamiltonian Dynamics

In this subsection, we present the Grams Hamiltonian dynamics, which builds upon the augmented Hamiltonian framework to analyze optimization algorithms. By leveraging this framework, we show that the Grams optimizer achieves a monotonic descent of the Hamiltonian and the loss function, with a descent speed that is provably equal to or faster than C-Adam. This highlights Grams' efficiency and robustness in dynamic optimization landscapes. The formal definition is provided below.

Definition 4.5 (Grams Hamiltonian Dynamics). *We could modify Hamiltonian dynamics,*

$$\begin{aligned}\frac{d}{dt} w_t &:= -\text{sign}(\nabla \mathcal{L}(w_t) \circ |\nabla \mathcal{K}(s_t)|) - \Phi_t(\nabla \mathcal{L}(w_t)) \\ \frac{d}{dt} s_t &:= \nabla \mathcal{L}(w_t) - \Psi_t(\nabla \mathcal{K}(s_t)),\end{aligned}$$

where $|\cdot|$ denotes element-wise absolute value, \circ is the Hadamard product, and Φ_t, Ψ_t are scaling functions.

The convergence properties of Grams within the Hamiltonian dynamics framework are formalized in the theorem below.

Theorem 4.6 (Convergence of Grams Hamiltonian Dynamics). *Following the dynamics in Definition 4.5, we have*

$$\begin{aligned}\Delta_H^{\text{Grams}}(w_t, s_t) &:= \frac{d}{dt} H(w_t, s_t) \leq 0, \\ \Delta_{\mathcal{L}}^{\text{Grams}}(w_t) &:= \frac{d}{dt} \mathcal{L}(w_t) \leq -\Delta_{\mathcal{L}}(w_t, s_t),\end{aligned}$$

where $\Delta_{H_t}(w_t, s_t)$ and $\Delta_{\mathcal{L}_t}(w_t, s_t)$ represent the decreasing rates of H and \mathcal{L} in accordance with the system in Definition 3.17.

Proof. Recall Eq. (6) and (7):

$$\begin{aligned}\Delta_H(w_t, s_t) &:= \langle \nabla \mathcal{L}(w_t), \Phi(\nabla \mathcal{L}(w_t)) \rangle + \langle \mathcal{K}(s_t), \Psi(\mathcal{K}(s_t)) \rangle \\ \Delta_{\mathcal{L}}(w_t, s_t) &:= \langle \nabla \mathcal{L}(w_t), \nabla \mathcal{K}(s_t) \rangle + \langle \nabla \mathcal{L}(w_t), \Phi_t(\nabla \mathcal{L}(w_t)) \rangle.\end{aligned}$$

Following the dynamics in Definition 4.5, we can calculate the derivative of $H(w_t, s_t)$ with respect to t :

$$\begin{aligned}
\Delta_H^{\text{Grams}}(w_t, s_t) &= \langle \nabla \mathcal{L}(w_t), \frac{d}{dt} w_t \rangle + \langle \nabla \mathcal{K}(s_t), \frac{d}{dt} s_t \rangle \\
&= \langle \nabla \mathcal{L}(w_t), -\text{sign}(\nabla \mathcal{L}(w_t)) \circ |\nabla \mathcal{K}(s_t)| - \Phi_t(\nabla \mathcal{L}(w_t)) \rangle \\
&\quad + \langle \mathcal{K}(s_t), \nabla \mathcal{L}(w_t) - \Psi_t(\nabla \mathcal{K}(s_t)) \rangle \\
&= \langle \nabla \mathcal{L}(w_t), -\text{sign}(\nabla \mathcal{L}(w_t)) \circ |\nabla \mathcal{K}(s_t)| \rangle + \langle \nabla \mathcal{K}(s_t), \nabla \mathcal{L}(w_t) \rangle - \langle \nabla \mathcal{L}(w_t), \Phi_t(\nabla \mathcal{L}(w_t)) \rangle \\
&\quad - \langle \nabla \mathcal{K}(s_t), \Psi_t(\nabla \mathcal{K}(s_t)) \rangle \\
&= \langle \nabla \mathcal{L}(w_t), \nabla \mathcal{K}(s_t) \rangle - \langle |\nabla \mathcal{L}(w_t)|, |\nabla \mathcal{L}(w_t)| \rangle - \Delta_H(w_t, s_t) \\
&\leq 0,
\end{aligned}$$

where the first step follows from the chain rule for the time derivative of the Hamiltonian H , the second step substitutes the dynamics from Definition 4.5, the third step separates the inner products for clearer analysis, the fourth step is following the definition of $\Delta H(w_t, s_t)$ and Lemma 3.5, and the last step follows Lemma 3.6, and $-\Delta H(w_t, s_t) \leq 0$.

Then, we calculate the derivative of $\mathcal{L}(w_t)$ with respect to t .

$$\begin{aligned}
\Delta_{\mathcal{L}}^{\text{Grams}}(w_t) &= \langle \nabla \mathcal{L}(w_t), -\text{sign}(\nabla \mathcal{L}(w_t)) \circ |\nabla \mathcal{K}(s_t)| - \Phi_t(\nabla \mathcal{L}(w_t)) \rangle \\
&= -\langle \nabla \mathcal{L}(w_t), -\text{sign}(\nabla \mathcal{L}(w_t)) \circ |\nabla \mathcal{K}(s_t)| \rangle - \langle \nabla \mathcal{L}(w_t), \Phi_t(\nabla \mathcal{L}(w_t)) \rangle \\
&= -\langle |\nabla \mathcal{L}(w_t)|, |\nabla \mathcal{L}(w_t)| \rangle - \langle \nabla \mathcal{L}(w_t), \Phi_t(\nabla \mathcal{L}(w_t)) \rangle \\
&= \langle \nabla \mathcal{L}(w_t), \nabla \mathcal{K}(s_t) \rangle - \langle |\nabla \mathcal{L}(w_t)|, |\nabla \mathcal{L}(w_t)| \rangle \\
&\quad - (\langle \nabla \mathcal{L}(w_t), \Phi_t(\nabla \mathcal{L}(w_t)) \rangle + \langle \nabla \mathcal{L}(w_t), \nabla \mathcal{K}(s_t) \rangle) \\
&= \langle \nabla \mathcal{L}(w_t), \nabla \mathcal{K}(s_t) \rangle - \langle |\nabla \mathcal{L}(w_t)|, |\nabla \mathcal{L}(w_t)| \rangle - \Delta_{\mathcal{L}}(w_t, s_t)
\end{aligned}$$

where the first step follows from the chain rule, the second step separated the inner products, the third step follows Lemma 3.5, the fourth step adds and subtracts the term $\langle \nabla \mathcal{L}(w_t), \nabla \mathcal{K}(s_t) \rangle$ simultaneously, the fifth step follows the definition of $\Delta_{\mathcal{L}}(w_t, s_t)$ from Eq. (2).

Since we know $\langle \nabla \mathcal{L}(w_t), \nabla \mathcal{K}(s_t) \rangle - \langle |\nabla \mathcal{L}(w_t)|, |\nabla \mathcal{L}(w_t)| \rangle \leq 0$,

$$\langle \nabla \mathcal{L}(w_t), \nabla \mathcal{K}(s_t) \rangle - \langle |\nabla \mathcal{L}(w_t)|, |\nabla \mathcal{L}(w_t)| \rangle \leq -\Delta_{\mathcal{L}}(w_t, s_t)$$

□

Based on this theorem, we compare the convergence rates of Grams and cautious optimizers in the context of Hamiltonian dynamics. The following theorem demonstrates that Grams achieves a faster or equal rate of loss descent compared to cautious optimizers, highlighting its efficiency in optimization.

Theorem 4.7 (Convergence Comparison of Hamiltonian Dynamics between Grams and Cautious Optimizers.). *From Theorem 4.6 and 3.16, recall $\Delta_{\mathcal{L}}^{\text{Grams}}(w_t)$ and $\Delta_{\mathcal{L}}^{\text{C}}(w_t, s_t)$:*

$$\Delta_{\mathcal{L}}^{\text{Grams}}(w_t) \leq \Delta_{\mathcal{L}}^{\text{C}}(w_t, s_t).$$

Proof. We calculate the difference between $\Delta_{\mathcal{L}}^{\text{Grams}}(w_t)$ and $\Delta_{\mathcal{L}}^{\text{C}}(w_t, s_t)$:

$$\Delta_{\mathcal{L}}^{\text{Grams}}(w_t) - \Delta_{\mathcal{L}}^{\text{C}}(w_t, s_t) = \langle \nabla \mathcal{L}(w_t), \nabla \mathcal{K}(s_t) \rangle - \langle |\nabla \mathcal{L}(w_t)|, |\nabla \mathcal{L}(w_t)| \rangle - \langle x_t, \mathbf{1} - \mathbf{1}_{x_t > 0} \rangle,$$

where $x_t = \nabla \mathcal{L}(w_t) \circ \nabla \mathcal{K}(s_t)$.

By applying Lemma 3.7, we know:

$$\langle \nabla \mathcal{L}(w_t), \nabla \mathcal{K}(s_t) \rangle - \langle |\nabla \mathcal{L}(w_t)|, |\nabla \mathcal{K}(s_t)| \rangle - \langle x_t, \mathbf{1} - \mathbf{1}_{x_t > 0} \rangle \leq 0,$$

with equality if all components of $\nabla \mathcal{L}(w_t) \circ \nabla \mathcal{K}(s_t) \geq 0$.

Thus:

$$\Delta_{\mathcal{L}}^{\text{Grams}}(w_t) - \Delta_{\mathcal{L}}^{\text{C}}(w_t, s_t) \leq 0,$$

which implies:

$$\Delta_{\mathcal{L}}^{\text{Grams}}(w_t) \leq \Delta_{\mathcal{L}}^{\text{C}}(w_t, s_t).$$

□

Remark 4.8. *Theorem 4.7 illustrates the faster loss decreasing speed in the Grams Hamiltonian dynamic system, compared to Cautious’s counterpart.*

Building on this comparison, we now state a corollary from [LCLL24] that establishes the convergence of bounded solutions in Hamiltonian systems to stationary points of the augmented loss.

Corollary 4.9 (Corollary 2.4 in [LCLL24]). *Assume that $\langle x, \Psi(x) \rangle \quad \forall x$ is positive definite, $\Psi(0) = 0$, and that $H(w, s) = \mathcal{L}(w) + \mathcal{K}(s)$ is differentiable. Then, the bounded solutions of the original system Eq. (5) converge to a stationary point of $H(w, s)$. Similarly, the bounded solutions of Definition 4.5 also converge to a stationary point of $H(w, s)$.*

4.4 Global Convergence of Grams

In this subsection, we establish the global convergence properties of the Grams optimizer. By analyzing the update rules and assumptions on the optimization landscape, we demonstrate that Grams converges to a stationary point of the objective function. This analysis underscores the optimizer’s robustness and effectiveness in a wide range of optimization scenarios.

4.4.1 Assumptions

To ensure theoretical rigor, we base our analysis on the following standard assumptions commonly used in optimization theory. These assumptions define the properties of the loss function and the optimization setting, enabling precise derivations of convergence guarantees.

Assumption 4.10 (Lower bound of loss). *The Loss function $\mathcal{L} : \mathbb{R}^d \rightarrow \mathbb{R}$ is differentiable and closed within its open domain $\text{dom}(\mathcal{L}) \subseteq \mathbb{R}^d$ and is bounded from below, i.e., $\mathcal{L}^* := \inf_w \mathcal{L}(w) > -\infty$.*

Assumption 4.11 (Bounded gradient). *The Loss function $\mathcal{L} : \mathbb{R}^d \rightarrow \mathbb{R}$ satisfies $\nabla \mathcal{L}(w) \leq G$ for all $w \in \text{dom}(\mathcal{L})$.*

Assumption 4.12 (L -smooth). *The Loss function $\mathcal{L} : \mathbb{R}^d \rightarrow \mathbb{R}$ is L -smooth for some $L > 0$.*

Assumption 4.13 (μ -PL-condition). *The Loss function $\mathcal{L} : \mathbb{R}^d \rightarrow \mathbb{R}$ satisfies μ -PL-condition for some $\mu > 0$.*

4.4.2 Convergence

In this subsection, we provide a detailed analysis of the convergence properties of the Grams optimizer. We begin by revisiting the convergence guarantee of the widely-used Adam optimizer as established in [LRJ23]. Using this as a foundation, we extend the analysis to Grams, highlighting its enhanced convergence behavior under the same assumptions.

Lemma 4.14 (Convergence of Adam, Section 5.3 in [LRJ23]). *Suppose that Assumptions 4.10, 4.11, and 4.12 hold. Given initial weight w_1 with initial optimality gap $\Delta_1 := \mathcal{L}(w_1) - \mathcal{L}^* < \infty$, choose an large enough G such that $G \geq \max\{\epsilon, 3\sqrt{L\Delta_1}\}$, a small enough fixed step size $\eta > 0$, and $\beta = \Theta(\eta G^{1/2})$. Consider that the weight w_t is updated by Adam (Algorithm 1) for each $t \in [T]$. Then we have*

$$\frac{1}{T} \sum_{t=1}^T \|\nabla \mathcal{L}(w_t)\|_2^2 \leq \frac{8G\Delta_1}{\eta T}.$$

The result in Lemma 4.14 establishes a baseline for the convergence of Adam under standard assumptions. Building on this, we extend the analysis to Grams by leveraging its unique update mechanism, which decouples the direction and magnitude of updates. The following theorem demonstrates that Grams achieves global convergence, meaning that it is guaranteed to reach the optimal objective value from any initial point with finite initial optimality gap.

Theorem 4.15 (Convergence of Grams). *Suppose that Assumptions 4.10, 4.11, 4.12 and 4.13 hold. Given initial point w_1 with initial optimality gap $\Delta_1 := \mathcal{L}(w_1) - \mathcal{L}^* < \infty$, choose large an enough G such that $G \geq \max\{\epsilon, 3\sqrt{L\Delta_1}\}$, a small enough fixed step size $\eta > 0$, and $\beta = \Theta(\eta G^{1/2})$. Consider that the weight w_t is updated by Grams (Algorithm 3) for each $t \in [T]$. Then we have*

$$\mathcal{L}(w_T) - \mathcal{L}^* \leq \frac{4G}{\mu\eta T} (\mathcal{L}(w_1) - \mathcal{L}^*).$$

Proof. Given initial weight w_1 , we denote w'_1, w'_2, \dots, w'_T be the weights updated by Adam where $w'_1 := w_1$. By Lemma 4.14, we have

$$\frac{1}{T} \sum_{t=1}^T \|\nabla \mathcal{L}(w'_t)\|_2^2 \leq \frac{8G\Delta_1}{\eta T}. \quad (14)$$

For each $t \in [T]$, we can show that

$$\begin{aligned} \|\nabla \mathcal{L}(w'_t)\|_2^2 &\geq 2\mu(\mathcal{L}(w'_t) - \mathcal{L}^*) \\ &= 2\mu(\mathcal{L}(w'_t) - \mathcal{L}(w'_{t-1}) + \mathcal{L}(w'_{t-1}) - \mathcal{L}(w'_{t-2}) + \dots + \mathcal{L}(w'_2) - \mathcal{L}(w'_1) + \mathcal{L}(w'_1) - \mathcal{L}^*) \\ &= 2\mu(\Delta \mathcal{L}_{w'_t, w'_{t-1}} + \Delta \mathcal{L}_{w'_{t-1}, w'_{t-2}} + \dots + \Delta \mathcal{L}_{w'_2, w'_1} + \mathcal{L}(w'_1) - \mathcal{L}^*) \\ &\geq 2\mu(\Delta \mathcal{L}_{w_t, w_{t-1}} + \Delta \mathcal{L}_{w_{t-1}, w_{t-2}} + \dots + \Delta \mathcal{L}_{w_2, w_1} + \mathcal{L}(w'_1) - \mathcal{L}^*) \\ &= 2\mu(\Delta \mathcal{L}_{w_t, w_{t-1}} + \Delta \mathcal{L}_{w_{t-1}, w_{t-2}} + \dots + \Delta \mathcal{L}_{w_2, w_1} + \mathcal{L}(w_1) - \mathcal{L}^*) \\ &\geq 2\mu(\mathcal{L}(w_t) - \mathcal{L}(w_{t-1}) + \mathcal{L}(w_{t-1}) - \mathcal{L}(w_{t-2}) + \dots + \mathcal{L}(w_2) - \mathcal{L}(w_1) + \mathcal{L}(w_1) - \mathcal{L}^*) \\ &= 2\mu(\mathcal{L}(w_t) - \mathcal{L}^*), \end{aligned} \quad (15)$$

where the first step follows from Assumption 4.13, the second step follows from basic algebra, the third step follows from Definition 3.14, the fourth step follows from Theorem 4.3, the fifth step

follows from $w'_1 = w_1$, the sixth step follows from Definition 3.14, and the last step follows from basic algebra.

Combining Eq. (14) and Eq. (15) gives

$$\mathcal{L}(w_T) - \mathcal{L}^* \leq \frac{4G}{\mu\eta T}(\mathcal{L}(w_1) - \mathcal{L}^*).$$

Thus we complete the proof. □

5 Empirical Experiments

We conducted comprehensive experiments across both pre-training and fine-tuning stages to evaluate the performance of our proposed Grams optimizer. Comparisons were made against several baseline optimizers, including Adam [KB14], Lion [CLH⁺24], C-Adam, C-Lion [LCLL24], and, in some experiments, RMSprop [HSS12, Rud16].

For Lion and C-Lion, we followed the recommendation from [CLH⁺24], setting their learning rates to $\frac{1}{10} \times$ Adam learning rate. Additional details and hyperparameters of our experiments can be found in Section A.

5.1 Pre-Training

We trained from scratch on the Llama 60M model [DJP⁺24] using the first 2,048,000 rows of data from English subset of the C4 dataset [RSR⁺20] to assess Grams’ optimization capability for Transformer-based [VSP⁺17] natural language generation (NLG) tasks. Due to the limited computing resources, we trained 1,000 steps using constant with warm-up scheduler, in order to simulate the beginning part of regular pre-training. We used the first 10,000 rows of validation data from the English section of the C4 dataset for evaluation. See Figure 2 for loss and Table 1 for evaluation results.

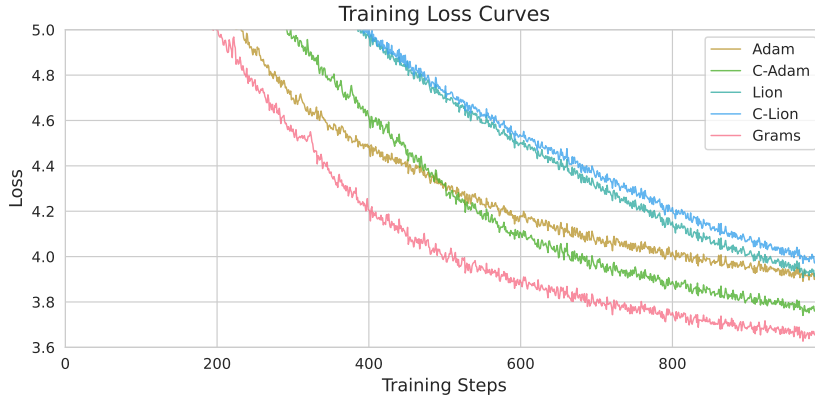


Figure 2: Loss curves of Llama 60M pre-training experiments.

The evaluation results of the Llama 60M pre-training experiments, as presented in Table 1, reveal that the Grams optimizer achieves the lowest perplexity (38.60) compared to other state-of-the-art optimizers, including Adam (49.83), C-Adam (43.21), Lion (50.25), and C-Lion (53.21). This substantial reduction in perplexity highlights the effectiveness of Grams in optimizing language model performance. While C-Adam and Lion exhibit improvements over their respective base

Optimizer	Perplexity↓
Adam	49.83
C-Adam	<u>43.21</u>
Lion	50.25
C-Lion	53.21
Grams	38.60

Table 1: Evaluation results of Llama 60M pre-training experiments.

optimizers, Adam and C-Lion, Grams outperforms all variants, underscoring its ability to enhance convergence and generalization. These results, in conjunction with the faster loss descent shown in Figure 2, demonstrate Grams’ superiority in both training efficiency and model quality for large-scale machine learning tasks.

For computer vision tasks, we trained and evaluated the WideResNet-50-2 model [ZK16] on the CIFAR-10 dataset [Kri09]. Figure 3 presents the training loss curves, and Table 2 provides the final accuracy results. See Figure 3 for loss curves.



Figure 3: Loss curves of WideResNet pre-training experiments. Smoothing is applied for clearer visualization.

Optimizer	Final Acc↑
RMSprop	84.47%
Adam	87.56%
C-Adam	88.78%
Lion	89.21%
C-Lion	89.42%
Grams	90.55%

Table 2: Evaluation results of WideResNet-50-2 training experiments from scratch.

Figure 3 and Table 2 highlight the performance of various optimizers—RMSprop, Adam, C-Adam, Lion, C-Lion, and Grams—on the WideResNet-50-2 model trained on the CIFAR-10 dataset. The training loss curves in Figure 3 show that Grams achieves the fastest and most consistent reduction in loss, outperforming the other optimizers. This rapid convergence is reflected in the final accuracy results presented in Table 2, where Grams achieves the highest accuracy of 90.55%,

surpassing Lion (89.21%), C-Lion (89.42%), Adam (87.56%) and C-Adam (88.78%). These results emphasize the effectiveness of Grams in accelerating optimization while achieving superior generalization, making it a robust choice for computer vision tasks.

5.2 Fine-Tuning

We performed full fine-tuning (FT) experiments on the Llama 3.2 1B model [DJP⁺24] using the MetaMathQA dataset [YJS⁺23]. To evaluate the model, we measured accuracy on the GSM-8K dataset [CKB⁺21]. Results are reported in Table 3.

Optimizer	GSM-8K \uparrow
Adam	48.90%
C-Adam	49.81%
Grams	51.02%

Table 3: Evaluation results of Llama 3.2 1B FT experiments.

The results in Table 3 showcase the performance of different optimizers during the full FT experiments on the Llama 3.2 1B model using the MetaMathQA dataset. The model’s accuracy was evaluated on the GSM-8K dataset. Among the optimizers, Grams achieved the highest accuracy of 51.02%, outperforming both Adam (48.90%) and C-Adam (49.81%). These results highlight the effectiveness of Grams in fine-tuning tasks, particularly in improving the model’s ability to handle complex datasets like GSM-8K. The superior performance of Grams demonstrates its capacity to achieve better generalization and optimization efficiency in fine-tuning scenarios.

We conducted parameter-efficient fine-tuning (PEFT) experiments on the Llama 3.2 3B model using the SORSA method [Cao24] and the first 100,000 rows of data from the MetaMathQA dataset [YJS⁺23]. The evaluation was performed on the MATH dataset [HBK⁺21], with the results summarized in Table 4.

Optimizer	MATH \uparrow
Adam	17.80%
C-Adam	16.62%
Grams	17.80%

Table 4: Evaluation results of Llama 3.2 3B PEFT experiments.

Grams achieved an accuracy of 17.80%, matching the performance of Adam and outperforming C-Adam (16.62%). These results indicate that Grams performs comparably to Adam in PEFT scenarios, maintaining its robust optimization capabilities while offering the additional benefits of parameter efficiency. This consistency further emphasizes Grams’ versatility in various fine-tuning settings.

6 Conclusion and Future Work

In this paper, we introduced Gradient Descent with Adaptive Momentum Scaling (Grams), a novel optimization algorithm designed to decouple the direction and magnitude of parameter updates. By leveraging this decoupling, Grams demonstrated superior performance in both theoretical convergence guarantees and empirical evaluations, outperforming state-of-the-art optimizers such as Adam [LH17], Lion [CLH⁺24], and their cautious variants [LCLL24]. The results across various

tasks highlight Grams’ potential as a transformative approach for efficient optimization in large-scale machine learning.

Grams achieved faster convergence and better generalization in our experiments. These properties make it particularly well-suited for modern applications such as large-scale pre-training and fine-tuning of deep learning models, where efficiency and stability are critical.

Building on the promising results of Grams, future work will focus on integrating ideas from recent advancements such as ADOPT [THM⁺24] and Schedule Free [DYM⁺24] optimization methods. Incorporating the ADOPT and schedule-free learning rate adjustment strategies might improve Grams’ robustness and performance across diverse tasks and architectures. By blending these complementary innovations with the core principles of Grams, we aim to develop an even more versatile and efficient optimization framework for large-scale machine learning challenges.

References

- [AAA⁺23] Josh Achiam, Steven Adler, Sandhini Agarwal, Lama Ahmad, Ilge Akkaya, Florencia Leoni Aleman, Diogo Almeida, Janko Altschmidt, Sam Altman, Shyamal Anadkat, et al. Gpt-4 technical report. *arXiv preprint arXiv:2303.08774*, 2023.
- [Ano24] Anonymous. Improving adaptive moment optimization via preconditioner diagonalization. In *Submitted to The Thirteenth International Conference on Learning Representations*, 2024. under review.
- [BWAA18] Jeremy Bernstein, Yu-Xiang Wang, Kamyar Azizzadenesheli, and Animashree Anandkumar. signsgd: Compressed optimisation for non-convex problems. In *International Conference on Machine Learning*, pages 560–569. PMLR, 2018.
- [Cao24] Yang Cao. Sorsa: Singular values and orthonormal regularized singular vectors adaptation of large language models. *arXiv preprint arXiv:2409.00055*, 2024.
- [CHG22] Xiangning Chen, Cho-Jui Hsieh, and Boqing Gong. When vision transformers outperform resnets without pre-training or strong data augmentations. In *International Conference on Learning Representations*, 2022.
- [CKB⁺21] Karl Cobbe, Vineet Kosaraju, Mohammad Bavarian, Mark Chen, Heewoo Jun, Lukasz Kaiser, Matthias Plappert, Jerry Tworek, Jacob Hilton, Reiichiro Nakano, Christopher Hesse, and John Schulman. Training verifiers to solve math word problems. *arXiv preprint arXiv:2110.14168*, 2021.
- [CLH⁺24] Xiangning Chen, Chen Liang, Da Huang, Esteban Real, Kaiyuan Wang, Hieu Pham, Xuanyi Dong, Thang Luong, Cho-Jui Hsieh, Yifeng Lu, et al. Symbolic discovery of optimization algorithms. *Advances in neural information processing systems*, 36, 2024.
- [DJP⁺24] Abhimanyu Dubey, Abhinav Jauhri, Abhinav Pandey, Abhishek Kadian, Ahmad Al-Dahle, Aiesha Letman, Akhil Mathur, Alan Schelten, Amy Yang, Angela Fan, et al. The llama 3 herd of models. *arXiv preprint arXiv:2407.21783*, 2024.
- [Doz16] Timothy Dozat. Incorporating nesterov momentum into adam, 2016.
- [DYM⁺24] Aaron Defazio, Xingyu Alice Yang, Harsh Mehta, Konstantin Mishchenko, Ahmed Khaled, and Ashok Cutkosky. The road less scheduled. *arXiv preprint arXiv:2405.15682*, 2024.

- [FKMN21] Pierre Foret, Ariel Kleiner, Hossein Mobahi, and Behnam Neyshabur. Sharpness-aware minimization for efficiently improving generalization. In *International Conference on Learning Representations*, 2021.
- [GKS18] Vineet Gupta, Tomer Koren, and Yoram Singer. Shampoo: Preconditioned stochastic tensor optimization. In *International Conference on Machine Learning*, pages 1842–1850. PMLR, 2018.
- [HBK⁺21] Dan Hendrycks, Collin Burns, Saurav Kadavath, Akul Arora, Steven Basart, Eric Tang, Dawn Song, and Jacob Steinhardt. Measuring mathematical problem solving with the math dataset. *arXiv preprint arXiv:2103.03874*, 2021.
- [HSS12] Geoffrey Hinton, Nitish Srivastava, and Kevin Swersky. Neural networks for machine learning lecture 6a overview of mini-batch gradient descent. *Cited on*, 14(8):2, 2012.
- [JNJ18] Chi Jin, Praneeth Netrapalli, and Michael I Jordan. Accelerated gradient descent escapes saddle points faster than gradient descent. In *Conference On Learning Theory*, pages 1042–1085. PMLR, 2018.
- [KB14] Diederik P. Kingma and Jimmy Ba. Adam: A method for stochastic optimization. *arXiv preprint arXiv:1412.6980*, 2014.
- [KBB15] Walid Krichene, Alexandre Bayen, and Peter L Bartlett. Accelerated mirror descent in continuous and discrete time. *Advances in neural information processing systems*, 28, 2015.
- [KMH⁺20] Jared Kaplan, Sam McCandlish, Tom Henighan, Tom B Brown, Benjamin Chess, Rewon Child, Scott Gray, Alec Radford, Jeffrey Wu, and Dario Amodei. Scaling laws for neural language models. *arXiv preprint arXiv:2001.08361*, 2020.
- [Kri09] Alex Krizhevsky. Learning multiple layers of features from tiny images, 2009.
- [LCLL24] Kaizhao Liang, Lizhang Chen, Bo Liu, and Qiang Liu. Cautious optimizers: Improving training with one line of code. *arXiv preprint arXiv:2411.16085*, 2024.
- [LH17] Ilya Loshchilov and Frank Hutter. Decoupled weight decay regularization. *arXiv preprint arXiv:1711.05101*, 2017.
- [LOG⁺19] Yinhan Liu, Myle Ott, Naman Goyal, Jingfei Du, Mandar Joshi, Danqi Chen, Omer Levy, Mike Lewis, Luke Zettlemoyer, and Veselin Stoyanov. Roberta: A robustly optimized bert pretraining approach. *arXiv preprint arXiv:1907.11692*, 364, 2019.
- [LRJ23] Haochuan Li, Alexander Rakhlin, and Ali Jadbabaie. Convergence of adam under relaxed assumptions. In *Proceedings of the 37th International Conference on Neural Information Processing Systems*, pages 52166–52196, 2023.
- [LYL⁺23] Kai Lv, Yuqing Yang, Tengxiao Liu, Qi jie Gao, Qipeng Guo, and Xipeng Qiu. Full parameter fine-tuning for large language models with limited resources. In *Annual Meeting of the Association for Computational Linguistics*, 2023.
- [MG15] James Martens and Roger Baker Grosse. Optimizing neural networks with kronecker-factored approximate curvature. In *International Conference on Machine Learning*, 2015.

- [MPT⁺18] Chris J Maddison, Daniel Paulin, Yee Whye Teh, Brendan O’Donoghue, and Arnaud Doucet. Hamiltonian descent methods. *arXiv preprint arXiv:1809.05042*, 2018.
- [NCLL24] Son Nguyen, Lizhang Chen, Bo Liu, and Qiang Liu. H-fac: Memory-efficient optimization with factorized hamiltonian descent. *arXiv preprint arXiv:2406.09958*, 2024.
- [Nes83] Yurii Evgen’evich Nesterov. A method for solving the convex programming problem with convergence rate $o(1/\kappa^2)$. In *Dokl. akad. nauk Sssr*, volume 269, pages 543–547, 1983.
- [NVL⁺17] Arvind Neelakantan, Luke Vilnis, Quoc V. Le, Lukasz Kaiser, Karol Kurach, Ilya Sutskever, and James Martens. Adding gradient noise improves learning for very deep networks, 2017.
- [RBL⁺22] Robin Rombach, Andreas Blattmann, Dominik Lorenz, Patrick Esser, and Björn Ommer. High-resolution image synthesis with latent diffusion models. In *Proceedings of the IEEE/CVF conference on computer vision and pattern recognition*, pages 10684–10695, 2022.
- [RSR⁺20] Colin Raffel, Noam Shazeer, Adam Roberts, Katherine Lee, Sharan Narang, Michael Matena, Yanqi Zhou, Wei Li, and Peter J Liu. Exploring the limits of transfer learning with a unified text-to-text transformer. *Journal of machine learning research*, 21(140):1–67, 2020.
- [Rud16] Sebastian Ruder. An overview of gradient descent optimization algorithms. *arXiv preprint arXiv:1609.04747*, 2016.
- [SMDH13] Ilya Sutskever, James Martens, George Dahl, and Geoffrey Hinton. On the importance of initialization and momentum in deep learning. In *International conference on machine learning*, pages 1139–1147. PMLR, 2013.
- [SS18] Noam Shazeer and Mitchell Stern. Adafactor: Adaptive learning rates with sublinear memory cost. In *International Conference on Machine Learning*, pages 4596–4604. PMLR, 2018.
- [THM⁺24] Shohei Taniguchi, Keno Harada, Gouki Minegishi, Yuta Oshima, Seong Cheol Jeong, Go Nagahara, Tomoshi Iiyama, Masahiro Suzuki, Yusuke Iwasawa, and Yutaka Matsuo. Adopt: Modified adam can converge with any β_2 with the optimal rate. *arXiv preprint arXiv:2411.02853*, 2024.
- [TLI⁺23] Hugo Touvron, Thibaut Lavril, Gautier Izacard, Xavier Martinet, Marie-Anne Lachaux, Timothée Lacroix, Baptiste Rozière, Naman Goyal, Eric Hambro, Faisal Azhar, et al. Llama: Open and efficient foundation language models. *arXiv preprint arXiv:2302.13971*, 2023.
- [TRRB23] Belinda Tzen, Anant Raj, Maxim Raginsky, and Francis Bach. Variational principles for mirror descent and mirror langevin dynamics. *IEEE Control Systems Letters*, 2023.
- [VMZ⁺24] Nikhil Vyas, Depen Morwani, Rosie Zhao, Itai Shapira, David Brandfonbrener, Lucas Janson, and Sham Kakade. Soap: Improving and stabilizing shampoo using adam. *arXiv preprint arXiv:2409.11321*, 2024.

- [VSP⁺17] Ashish Vaswani, Noam Shazeer, Niki Parmar, Jakob Uszkoreit, Llion Jones, Aidan N. Gomez, Lukasz Kaiser, and Illia Polosukhin. Attention is all you need. *Advances in Neural Information Processing Systems*, 2017.
- [WRJ16] Ashia C Wilson, Benjamin Recht, and Michael I Jordan. A lyapunov analysis of momentum methods in optimization. *arXiv preprint arXiv:1611.02635*, 2016.
- [XZL⁺24] Xingyu Xie, Pan Zhou, Huan Li, Zhouchen Lin, and Shuicheng Yan. Adan: Adaptive nesterov momentum algorithm for faster optimizing deep models. *IEEE Transactions on Pattern Analysis and Machine Intelligence*, 2024.
- [YJS⁺23] Longhui Yu, Weisen Jiang, Han Shi, Jincheng Yu, Zhengying Liu, Yu Zhang, James T Kwok, Zhenguo Li, Adrian Weller, and Weiyang Liu. Metamath: Bootstrap your own mathematical questions for large language models. *arXiv preprint arXiv:2309.12284*, 2023.
- [ZK16] Sergey Zagoruyko and Nikos Komodakis. Wide residual networks. In *Proceedings of the British Machine Vision Conference 2016*, 2016.
- [ZTD⁺20] Juntang Zhuang, Tommy Tang, Yifan Ding, Sekhar C Tatikonda, Nicha Dvornek, Xenophon Papademetris, and James Duncan. Adabelief optimizer: Adapting step-sizes by the belief in observed gradients. *Advances in neural information processing systems*, 33:18795–18806, 2020.
- [ZZC⁺24] Jiawei Zhao, Zhenyu (Allen) Zhang, Beidi Chen, Zhangyang Wang, Anima Anandkumar, and Yuandong Tian. Galore: Memory-efficient llm training by gradient low-rank projection. *ArXiv*, abs/2403.03507, 2024.

A Experiments Details

For the Lion and C-Lion optimizers, we set the learning rate to $\frac{1}{10} \times$ Adam learning rate, as recommended in [CLH+24].

A.1 Pre-Training

For the pre-training experiments with Llama 3.2 60M [DJP+24], we used the first 2,048,000 rows of training data from the English section of the C4 dataset [RSR+20]. We used the first 10,000 rows of validation data from the English section of the C4 dataset for evaluation. Table 5 provides a detailed summary of the hyperparameters employed.

Optimizers	Grams/AdamW/CAdamW	Lion/CLion
Training		
Epoch	1	1
Learning Rate	6e-3	6e-4
Weight Decay	0.0	0.0
Batch Size	2048	2048
Model Precision	BF16	BF16
Mix Precision	BF16&TF32	BF16&TF32
Scheduler	Constant with warm-up	Constant with warm-up
Warm-up Steps	50	50
Grad Clipping	1.0	1.0
β_1	0.9	0.9
β_2	0.95	0.95
ϵ	1e-6	1e-6
Seq-len	256	256
Evaluating		
Precision	BF16	
Seq-len	256	

Table 5: Hyperparameters for Llama 3.2 60M pre-training experiments.

For the computer vision experiments, we used the CIFAR-10 dataset [Kri09] to train and evaluate the WideResNet-50-2 model [ZK16]. Table 6 outlines the corresponding hyperparameters.

A.2 Fine-Tuning

For fine-tuning experiments of the Llama 3.2 1B model, Table 7 provides the detailed hyperparameters.

For PEFT of the Llama 3.2 3B model, Table 7 provides the detailed hyperparameters.

Optimizers	Grams/AdamW/CAdamW	Lion/CLion
Training		
Epoch	10	10
Learning Rate	2e-3	2e-4
Weight Decay	0.0	0.0
Batch Size	128	128
Model Precision	FP32	FP32
Mix Precision	None	None
Scheduler	Linear	Linear
Warm-up Steps	100	100
Grad Clipping	1.0	1.0
β_1	0.9	0.9
β_2	0.999	0.99
ϵ	1e-6	1e-6
Evaluating		
Precision	FP32	

Table 6: Hyperparameters for WideResNet-50-2 pre-training experiments.

Optimizers	Grams/AdamW/CAdamW
Training	
Epoch	1
Learning Rate	1e-4
Weight Decay	0.0
Batch Size	64
Model Precision	BF16
Mix Precision	BF16&TF32
Scheduler	Cosine
Warm-up Ratio	0.03
Grad Clipping	1.0
β_1	0.9
β_2	0.999
ϵ	1e-6
Seq-len	512
Evaluating	
Precision	BF16
Seq-len	1024

Table 7: Hyperparameters for Llama 3.2 1B fine-tuning experiments.

Optimizers	Grams/AdamW/CAAdamW
Training	
Epoch	1
Learning Rate	1e-4
Weight Decay	0.0
Batch Size	128
Model Precision	BF16
Mix Precision	BF16&TF32
Scheduler	Cosine
Warm-up Ratio	0.03
Grad Clipping	1.0
β_1	0.9
β_2	0.999
ϵ	1e-6
Seq-len	512
Rank	128
SORSA [Cao24] γ	1e-3
Evaluating	
Precision	BF16
Seq-len	2048

Table 8: Hyperparameters for Llama 3.2 3B PEFT experiments.